Article

Not peer-reviewed version

Biophysics vs. Biochemistry in Nanopharmacy: The Second (SD-C_{60}) and Third (TD-C_{60}) Derivatives of Fullerene C_{60}

Djuro Koruga * , Dietmar Kuhn , Lidija Matija , Ivana Stanković , Aleksandra Dinić

Posted Date: 17 March 2025

doi: 10.20944/preprints202503.1142.v1

Keywords: hydrogen bonds; water; DNA; proteins; fullerene C60 derivatives; FTIR; TEM; AFM/MFM; biophysical nanopharmacy

 doi:10.20944/preprints202503.1142.v1

Article

Biophysics vs. Biochemistry in Nanopharmacy: The Second (SD-C_{60}) and Third (TD-C_{60}) Derivatives of Fullerene C_{60}

Djuro Koruga [1,2,*], Dietmar Kuhn [3], Lidija Matija [1], Ivana Stanković [1] and Aleksandra Dinić [1]

[1] NanoLab, Biomedical Engineering, Faculty of Mechanical Engineering, University of Belgrade, 11120 Belgrade, Serbia; lmatija@mas.bg.ac.rs (L.M.); imimeusnic@mas.bg.ac.rs (I.S.); adinic@mas.bg.ac.rs (A.D.)

[2] NanoWorld, 11043 Belgrade, Serbia; djuro.koruga@gmail.com

[3] LAUS GmbH, 67489 Kirrweiler, Germany; Dietmar.Kuhn@laus.de

* Correspondence: dkoruga@mas.bg.ac.rs or djuro.koruga@gmail.com; Tel.: +38163287353

Abstract: Objectives: Today's pharmacy and its application in medicine, including the current nanotechnological approach, is based on the biochemical laws of covalent bonds. Due to their changed chemical potential, most nanosubstances, compared to classical ones, as well as tissue penetration, have distinct toxic properties. To overcome the negative effects of the biochemical application of nano-substances in medicine, using the example of fullerene C_{60} and its derivatives, we show that their biophysical effect is possible through non-covalent hydrogen bonds; **Methods:** In the first step, we used the molecule C_{60}, which is very poorly soluble in water and toxic under certain conditions, and then we added C_{60} with 36 OH groups (first derivative, FD-C60 or fullerol) with increased water solubility and reduced toxicity. To reduce higher toxicity and increase solubility and effect, fullerol in solution was exposed to an oscillatory electromagnetic field with *Re* (real) and *Im* (imaginary) parts. Three to nine stable water layers around the fullerol are formed when *Re* part of the electromagnetic field is used (second derivative, SD-C_{60} or 3HFWC). However, in addition to SD-C_{60}, ordered water chains and bubbling of water in the solution (third derivative, TD-C_{60}) are formed when both *Re* and *Im* part of the external electromagnetic field are applied. **Results:** A comparative structural and physicochemical characterization of fullerene C_{60} and its derivatives was performed. Fullerene C_{60} and fullerol (FD-C_{60}) interact with biological structures biochemically, while the second (SD-C_{60}) and third (TD-C_{60}) derivatives act biophysically via hydrogen bond oscillation. The paper explains the mechanism of action of SD-C_{60} and TD-C_{60} via hydrogen bonds and gives examples of biomedical applications citing our published experimental results. **Conclusions:** This study shows that the Yin-Yang machinery, based on the nanophysics of non-covalent hydrogen bonds, is possible and that the first attempt has been made to establish nanomedicine based on non-covalent hydrogen bonds of water, DNA and proteins.

Keywords: hydrogen bonds; water; DNA; proteins; fullerene C_{60} derivatives; FTIR; TEM; AFM/MFM; biophysical nanopharmacy

1. Introduction

The first potential of nanopharmacy in medical and pharmaceutical uses is through its application in the delivery of existing therapeutic and diagnostic agents. Today's nanopharmacology deals with the application of nanoscience and nanotechnology based on new pharmacological principles with the aim of increasing therapeutic effectiveness and reducing side effects, as well as achieving targeted delivery of the drug to specific locations in a controlled manner. Nanocarriers such as liposomes, nanoparticles, nanostructured lipid carriers, polymer micelles, and polymer conjugates of drugs with a size of 200 nm show promising effectiveness in the field of medicine.

 doi:10.20944/preprints202503.1142.v1

However, there is a lack of data on clinical studies and the usefulness of DDS (drug delivery system) in patients. Pharmacologists must be involved in the investigation of pharmacokinetics and pharmacodynamics of DDS if the products have reached clinical use [1–3].

Since discovering the right biomarkers to target for a certain disease is a key challenge for medical research, the second potential of nanopharmacy in medical and pharmaceutical use is if nanoparticles are replaced with nanomaterials, which symmetry are similar to biological water and biomolecules. Bearing in mind that the energy states (electronic, vibrational, rotation, and translation) of materials are defined by their symmetry pharmaceutical nanomaterials will have greater efficiency than nanoparticules in biomedicine. One of the examples of nanomaterials that have elements of icosahedral symmetry, such as biological water, and some biomolecules such as collagen, microtubules, and clathrin, is the C_{60} fullerene molecule. To overcome the problems of solubility of C_{60} molecules in water and its toxicity, the first derivative (FD-C_{60} or fullerenol) was made. Molecule C_{60} is added with different numbers of OH groups by covalent bonds. Many studies of the use of FD-C_{60} have been carried out in biomedical research and it has been shown that it has good effects at certain concentrations in photoinduced DNA, to inhibitHIV-1 protease, generate specific interaction with proteins (fullerene specific antibodies), skin effects, nerve protection, antitumor activity and others [4]. It has been shown that the toxicity of C_{60} is reduced by about 50% if OH groups are added [5]. Fullerene hydroxylation increases water solubility and affects how these nanomaterials interact with biological systems. It has been demonstrated that increasing fullerene water solubility through surface modification is related to significantly decreased toxicity. Specifically, this study observed decreased toxicity of hydroxylated fullerene compared to the cytotoxic effects of fullerene aggregates in human skin (HDP) and liver carcinoma (HepG2) cells [5]. Similarly, it was observed that hydroxylation decreases the toxic potential of fullerene in mouse L929 fibro sarcoma, rat C6 glioma, and U251 human glioma cell lines [6]. Additionally, hydroxylated fullerene induced apoptotic changes in the investigated cell lines, while fullerene C_{60} induced necrotic cell death. The distinct effects of pristine and modified fullerene originate from the different nanoparticle interactions with the intracellular metabolic pathways [5,6]. The beneficial effects of fullerenol are well documented. In human breast cancer cell lines, $C_{60}(OH)_{22}$ inhibited cancer cell growth and suppressed doxorubicin-induced cytotoxicity [7]. Fullerenol $C_{60}(OH)_{20}$ (FD-C_{60}) showed antitumor and anti-metastatic activity in vitro and in vivo EMT-6 breast cancer metastasis model [8]. The anti-tumor effect of fullerenol $C_{60}(OH)_{20}$ may be exerted through its effects on oxidative stress status, inhibition of the formation of angiogenesis factors, or through modulation of the immune profile [9]. However, fullerene hydroxylation did not provide the absolute absence of toxicity in living systems [10,11].

In both cases, the first and second potential of nanopharmacy, biological water was the environment in which nanopharmaceutical substances (nanoparticles and nanomaterials) acted. The first derivative of C_{60} (FD-C60 or fullerenol) belongs to the group of biochemical substances, while our approach to the second and third derivative of C_{60} (SD-C_{60} and TD-C_{60}) belongs to the group of biophysical substances. The basic differences between the biochemical and biophysical properties of C_{60} derivatives are given in discusion. In our approach, the third potential of nanopharmacy in biomedicine is, that water is not only an environment in which biochemical processes take place but is also an active factor in biophysical processes that are realized through covalent and non-covalent hydrogen bonds oscillations. In our research, we applied biomimmicry, the principles of symmetry and harmony to the functioning of water, DNA, and proteins based on the oscillatory processes of their hydrogen bonds. As non-covalent hydrogen bonds have classical and quantum properties [12], and as the C_{60} molecule has a *Re* (real) and *Im* (imaginary) electromagnetic spectrum [13], a method was developed to obtain the second derivative of the C_{60} molecule (SD-C_{60} or 3HFWC) as a result of the effect of the *Re* spectrum of the external electromagnetic oscillatory field and *Re* spectra of C_{60} on water around the FD-C_{60}. In such a process, stable water layers are formed around FD-C_{60} [14–17]. However, when there is the effect of the *Re* and *Im* spectra of the external electromagnetic oscillatory field and the effect of the *Re* and *Im* spectra of C_{60} on the FD-C_{60} and water in the reactor, stable water layers are formed around FD-C_{60} (SD-C_{60} or 3HFWC), and stable water “helix chains” and water

 doi:10.20944/preprints202503.1142.v1

bubbles ("micelles") are formed in the reactor (TD-C_{60} or 3HFWC-W). The effects of the third potential of nanopharmacy (SD-C_{60} and TD-C_{60}) in biomedical research on the treatment of skin cancer, Alzheimer's, pain, and memory in mice are presented based on this paper. However, this third approach to nanopharmacy (SD-C_{60} and TD-C_{60}) opens up the possibility of a new approach to personal medicine because it accesses the functionality of DNA and proteins through a biophysical energy-informational approach of hydrogen bonds that is specific for each individual. Biophysical nanopharmacy based on hydrogen bonds of DNA, proteins, and water may play a pivotal role in advancing personalized medicine by providing innovative tools and platforms for precise diagnosis, targeted therapy, and monitoring of treatment responses.

2. Materials and Methods

2.1. Sample Preparation

The two basic materials used in this experiment are water and the fullerenol C60(OH)36) or FD-C60. Tap water was treated using reverse osmose and finally the composition of the water in experiment was: Ca^{2+}—0.60 mg/L, Mg^{2+}—0.53 mg/L, Na^{+}—0.32 mg/L, K^{+}–0.04mg/L, $Fe^{2+/3+}$—<0.005mg/L, NH_4^{+}—<0.03,Cl—0.18mg/L and NO_3—0.12mg/L, with a conductivity in the tank of 0.05 mS/cm, Water with this characteristic was used for production both SD-C_{60} and TD-C_{60}. More information about water and its hydrogen bonds properties can be found in papers [16,17] and Supplement S1. As a precursor of SD-C60, the fullerenol C60(OH)36 or FD-C60, with a molecular weight of 1332 Da, a dust composition (yellow color), and a purity of 99.99% was ordered in a dark bottle from Solaris Chem, Vaudreuil-Dorion, QC, Canada. It was stored until use in a dark room, with a humidity of 35 ± 2% and a temperature of 20 ± 2 °C.

The C60 derivatives was synthesized at the NanoWorld Lab and TFT Nano Center, Belgrade, Serbia (3 g of fullerol was mixed with 20 L of ultra-pure water), according to the patented procedure [14,15]. The formation of C60 derivate began with 0.150 g/L of C60(OH)36 dissolved in high-purity water (0.05 μS/cm) under the influence of an external oscillatory magnetic field +250/−92 mT [$H(\omega t) = Acos(\omega t) + Bisin(\omega t)$] according to the icosahedral eigenvalues T1u, T_{1g}, T2u, T_{2g} (Fibonacci numbers ±Φ and, ±ϕ,) Supplement S2. At the same time, under the internal action of the vibrations energies of the C60 molecules (same vibration law as an external *Re* and *Im* magnetic fields) in a reactor at 37 °C, the formation of a few C_{60} derivatives was realized (Figure 1).

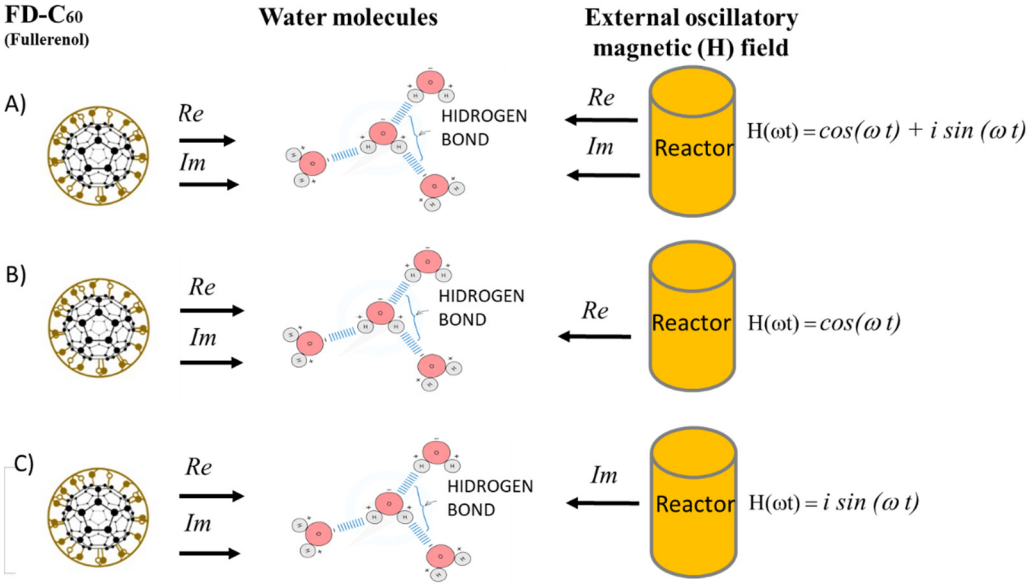

Figure 1. The method of production of C_{60} derivatives (SD-C_{60} and TD-C_{60}) according to the principle "between a hammer and an anvil" in the frequency domain. In this process, water molecules are located between two electromagnetic fields of action: The C_{60} molecule and the external one (reactor). The C_{60} molecule has its natural

 doi:10.20944/preprints202503.1142.v1

permanent *Re* and *Im* electromagnetic effect (Supplement S3) on the water molecules in its environment. The external effect (reactor) can be selective: A) both *Re, Im,* B) *Re,* and C) *Im* part. Depending on which combinations of *Re* and *Im* are realized, there will be different organizations of water molecules in layers.

2.2. Sample Characterization

Investigations of C60 derivatives were characterized using UV-VIS-NIR, FTIR TEM/STEM, and AFM/MFM techniques.

2.2.1. UV–Vis–NIR and FTIR

UV–Vis–NIR characterization of C_{60} derivatives was performed using a Lambda 500 spectrometer, Perkin-Elmer, USA, in the range of 250–3000 nm. FTIR characterization was performed using the Spectrum Spotlight 400 FTIR Imaging System, Perkin-Elmer, Waltham, MA, USA, in the range of 2,500–16,000 nm.

2.2.2. TEM and HAADF-STEM

TEM (transmission electron microscopy) analysis of the dry particles of C_{60} derivatives was performed in order to determine their solid-state size and shape. The samples in a liquid state were applied to the TEM copper mash coated with carbon and dried in air. After drying the samples, they were analyzed and recorded in three TEM laboratories: (1) the CM12 Philips/FEI Transmission Electron Microscopy, Eindhoven, the Netherlands, magnification ×45,000 and ×60,000; (2) TEM, JEM 1400, JEOL, Tokyo, Japan, magnification ×120,000 up to ×200,000; and (3) High-Angle Annular Dark Field Scanning Transmission Electron Microscopy (HAADF-STEM), Thermo-Fisher Talos/Osiris 200 kV (Waltham, MA, USA), Zeiss Libra (Oberkochen, Germany) 120 kV, 200 kV electron energy, STEM mode with bright field, with evaluation software Thermo-Fisher Velox 3.7 and energy- dispersive X-ray analysis EDXS mapping = ChemiSTEM, with Z > 8 installed.

2.2.3. AFM/MFM

Samples of C_{60} derivatives were characterized using JSPM-5200, Scanning Probe Microscopy, JEOL, Japan. Two methods were used: (1) AFM (Atomic Force Microscopy), and (2) MFM (Magnetic Force Microscopy). Both techniques are non-invasive. AFM method is based on Van der Waal's forces and London-type dispersive forces between tip and sample, while MFM, in the non-contact imaging mode, is based on magnetic dipole-dipole interaction (hydrogen bonds) between tip and sample (measuring deflection of tip "ϕ" in deg.). For magnetic gradient investigation, specialized cantilevers, type HQ NSC18/Co-CrAl BS (MikroMasch, Tallinn, Estonia), with force constants in the range between 1.2 and 5.5 N/m and with the resonant frequency range between 60 and 90 kHz, were used. The scanning size of the sample depended on the object size and number of objects that should be scanned. In this case, the optimal scan size should be between 10 nm and 100 nm.

2.3. Methods

2.3.1. Symmetry

The symmetry of the structure will determine its energy states (electronic, vibrational, and rotational). Since C60 is a molecular crystal with icosahedral symmetry, it will transmit its vibrational effects through hydrogen bonds into the surrounding water space. When water arranges itself into water chains or clusters, it also does so according to the laws of symmetry. Biomolecules that contain hydrogen bonds in their structure, such as DNA, collagen, microtubules, clathrin, and other proteins, are complex symmetrical objects. However, what they all have in common are the identical electronic and vibrational states of covalent (molecular, O-H and N-H) and non-covalent (intermolecular O...H and N...H) hydrogen bonds. Because of this, it is possible to transmit signals from one, to another, to

 doi:10.20944/preprints202503.1142.v1

a third object. In our case, it is the transmission of vibrational signals from derivatives of C_{60} molecules through water to biomolecules such as DNA, collagen, microtubules, clathrin, etc.

2.3.2. Harmony

The key element for achieving harmony in hydrogen bonds, and thus also achieving the optimal conformational state of biomolecules, is the ratio of covalent (O-H or N-H) and non-covalent (O...H or N... O) hydrogen bonds. Experimentally, using neutron diffraction, it was determined that the value of O-H vs O...H is within the limits of 1.2 to 2.1. [18]) . However, the optimal (harmonic) value is around 1.62 [16]. In order for the conformational states of biomolecules to be optimal, that is, for biological water to perform an optimal function (good interaction with biomolecules), the value of O-H/O...H should be around 1.61803.

2.3.3. Perfection

This third element of the method, perfection, which is based on the laws of perfect numbers, is not relevant to this research, which takes into account the individual interactions of C_{60} molecule derivatives (SD-C_{60} and TD-C_{60}) with water and biomolecules. But this element of the method is very significant if the effect of C_{60} molecule derivatives on the whole organism is taken into account. The reason for this lies in the fact that the creation of an organism from a fertilized egg cell (embryogenesis) to its arrival in the world takes place according to the laws of body symmetry, the harmony of the formation and organization of cells in tissues and organs, and the creation of the body's biophysical information networks (quantum-classical) and codes according to the laws of perfect numbers [19].

A schematic representation of the SHP (*symmetry-harmony-perfection*) method and its connection with the structures considered in this work (derivatives of C_{60} molecules, DNA, proteins, and water) from the aspect of hydrogen bonds is given in Figure 2.

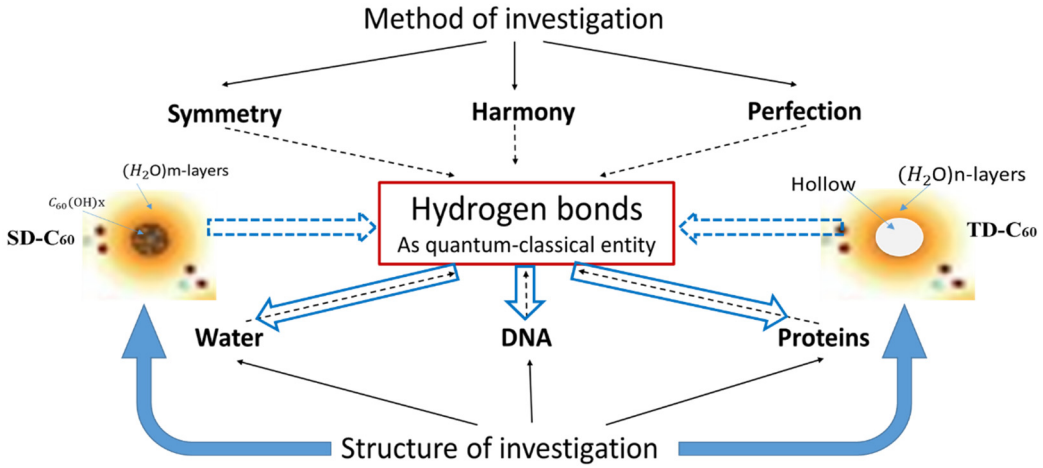

Figure 2. Schematic representation of the object of research (hydrogen bonds in DNA, proteins, and water) and the method of obtaining C_{60} derivatives (SD-C_{60} and TD-C_{60}) with hydrogen bonds and their influence on DNA, proteins, and water. Solid and dashed black lines show functional dependencies between method and material, while blue arrows show the effect of newly created nanopharmaceutical materials (SD-C_{60} and TD-C_{60}) on hydrogen bonds of DNA, proteins, and water. In this method, water is not only a medium in which processes take place, but its **hydrogen bonds are** an active participant in the process. The importance of hydrogen bonds for the functioning of the organism was first noticed in 1939 by Lines Pauling, who said "I believe that as the methods of structural chemistry are further applied to physiological problems, it will be found that the significance of the hydrogen bonds for physiology is greater than that of any other single structural feature"

 doi:10.20944/preprints202503.1142.v1

3. Results

3.1. FD-C₆₀ (the First Derivative of the C₆₀)

In the experiment five different structures of C_{60} derivatives are obtained, which are shown in Figures 3–6. Figure 3 shows the first derivative of the C_{60} molecule (FD-C_{60}), size 1.2 nm in the form of a schematic representation (a), TEM image (b) and in solution (c) (0.15 g/L dissolved in water is medium brown in color). Physicochemical characteristics of FD-C_{60} are presented in reference [17].

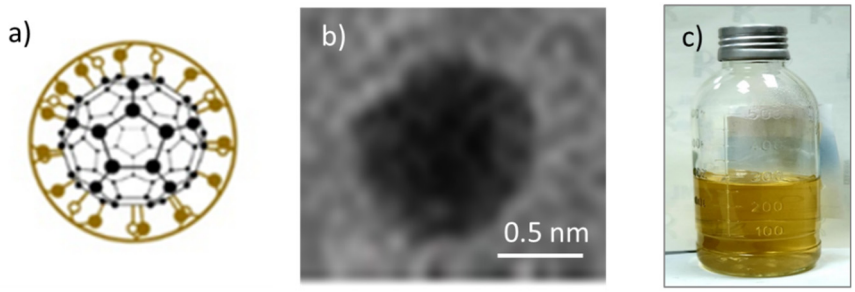

Figure 3. FD-C_{60} (fullerenol) is composed of molecule C_{60} and 36 OH groups attached by covalent bonds. In a solid dry state, it is 1.2 nm in size, while under the influence of moisture, it is about 1.6-1.8 nm. It dissolves well in water and, depending on the concentration, is dark to light brown.

3.2. TEM Images of SD-C₆₀ and TD-C₆₀ Derivatives of C₆₀

There are three types of SD-C_{60}, depending on the type of oscillatory magnetic field used to form water layers around FD-C_{60} (as a precursor) and water chains that are formed in the water solution of the reactor. If an oscillating magnetic field of the type $H(\omega t)=cos(\omega t)+isin(\omega t)$ is applied, then we get the first type of the second derivative C_{60}: SD-C_{60}, which we marked in previous works as 3HFWC, which we will now mark as SD-C_{60}-(f), where $f=\omega/2\pi$ (Figure 4). However, if we apply an oscillatory magnetic field of the type $H(\omega t)=cos(\omega t)$, then due to the nature of the field in the frequency domain the two solutions $f_1=1/2\ e^{i\omega t}$ (positive frequency) and $-f_1=1/2\ e^{-i\omega t}$ (negative frequency). Two structures of the second derivative C_{60} are formed: SD-C_{60}-(f_1) and SD-C_{60}-($-f_1$), which are mixed and which in previous works we marked 3HFWC-W. Notation (f_1) and ($-f_1$) means that the structures originate from the *Re* (real) spectrum of the oscillatory magnetic fields (C_{60} and reactor). Until now, only the structure SD-C_{60}-(f_1) has been observed, which we identified with SD-C_{60}-(f) because they are the same structures in character, only differing in the number of water layers (Figure 5a) However, if an oscillatory magnetic field of the type $H(\omega t)= isin(\omega t)$ is applied, then due to the character of the field a third derivative C_{60} (TD-C_{60}) is formed with two water structures TD-C_{60}-(f_1^*) and TD -C_{60}-($-f_1^*$) (Figure 6). They are the result of the composition of the *Im* (imaginary) spectrum of the oscillatory magnetic field of the reactor and the imaginary spectrum C_{60}.

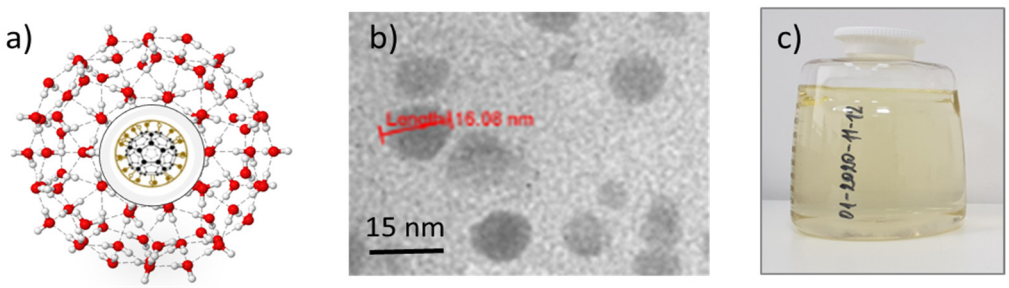

Figure 4. SD-C_{60}-(f) [3HFWC]: a) The structure consists of C_{60} molecules to which OH groups are connected by covalent bonds and water layers where the water molecules are arranged according to 3D Penrose tiling (3DPT) [16] b) TEM Image of SD-C_{60}-f different size, from 9-16 nm, c) the color of the derivative will depend on the

 doi:10.20944/preprints202503.1142.v1

percentage of success in creating water layers around the precursor (FD-C_{60}, fullerenol). When comparing the colors of the products from Figure 3c and Figure 4c (which contain the same percentage of fullerenol), it can be seen that the product in Figure 4c is much lighter than in Figure 3c, which means that the greater part (about 85%) of the fullerol is enriched with water layers, i.e., that the transformation of FD-C_{60} into SD-C_{60}-(f) was successfully completed.

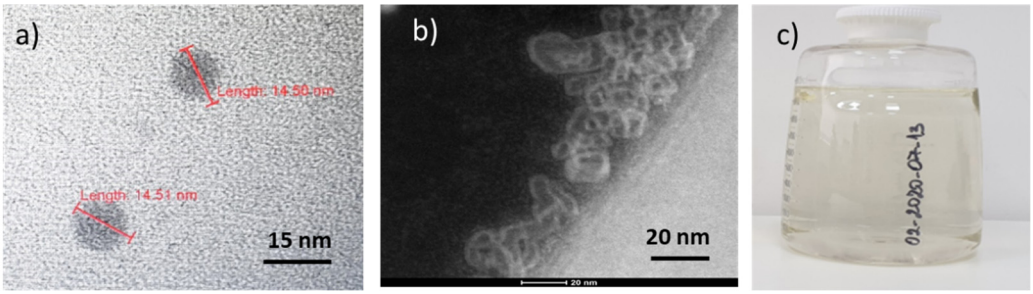

Figure 5. SD-C_{60}-(f_1,-f_1) [3HFWC-W] is formed under the influence of the oscillatory magnetic field H(ωt)=cos(ωt). Two types of structures, "a" and "b", are formed and identified by TEM. Structure "a" is formed as a consequence of frequency $f_1=1/2e^{i\omega t}$ and is similar to SD-C_{60}-(f) (Figure 4a) because they originate from the Re spectrum of C_{60} and the reactor. The difference between f and f_1 structures can be in the number of layers (size). The structure f_1 is of the same size (about 15 nm) while f_1 can be up to 30 nm in size. Water chain structure "b" is formed under the influence of frequency $-f_1=1/2e^{-i\omega t}$ (negative frequency of the Re spectrum of the reactor and C_{60}). Due to the significantly lower content of SD-C_{60}-(f_1) and the higher water content of SD-C_{60}-(-f_1), this complex (f_1/-f_1) has a much lighter brown color than structure f (Figure 4c).

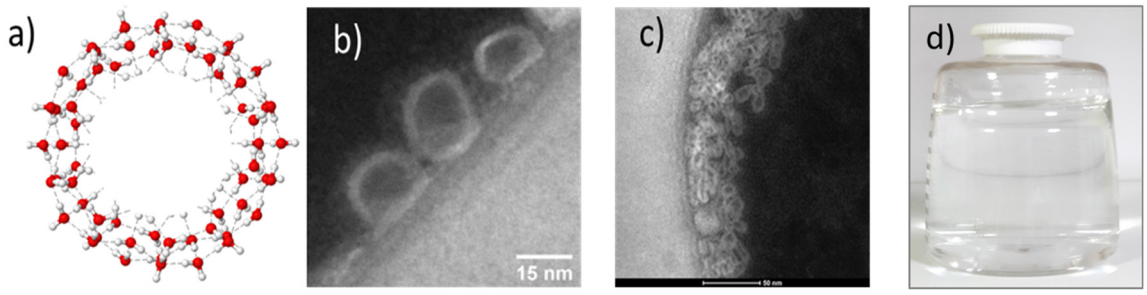

Figure 6. TD-C_{60}-(f_1^*,-f_1^*) is formed under the influence of the oscillatory magnetic field H(ωt)=isin(ωt). Two types of water structures are formed. Structure "a"/"b" (a closed single cycle arranged according to 3D Penrose tiling) is formed as a consequence of frequencies $f_1^*=e^{i\omega t}/2i$, while structuring "c" (a complex of closed cyclic water structures and open linear chain water structures) is formed under the influence of frequency $-f_1^*=-e^{-i\omega t}/2i$. Even if "b" and "c" do not contain the material structure of C_{60} molecules, these structures belong to C_{60} derivatives because they were created under the influence of Im (imaginary) C_{60} spectra and the reactor frequencies $f_1^*=e^{i\omega t}/2i$ and $-f_1^*=-e^{-i\omega t}/2i$. As TD-$C_{60}$ is a substance composed of ordered clusters of water molecules found in ordinary water (unstructured), its color is white and transparent (d).

3.3. FTIR Spectra of SD-C_{60} and TD-C_{60} Derivatives of C_{60}

The FTIR spectrum, *Re* and *Im*, of the C_{60} molecule is well-known [13] (Supplement S3). The FTIR spectrums of FD-C_{60} and SD-C_{60}-(f) were also performed, and the diagrams show significant differences in the 3000-3300 nm domain where hydrogen bonds are dominant [16]. In this paper, we have presented the spectrum of SD-C_{60}-(f), Figure 7, [17] so that it could be compared with the performed FTIR spectra for SD-C_{60}-(f_1,-f_1) (Figure 8) and TD-C_{60}-(f_1^x,-f_1^x)(Figure 9).

As can be seen from the diagram (Figures 7–9), there are great similarities in the spectra as well as small differences. This indicates that the structures are of the same symmetry in all three cases. In other words, aqueous layers where the C_{60} molecule is physically present and aqueous layers where the C_{60} molecule is not physically present oscillate approximately the same. The position of the peaks

 doi:10.20944/preprints202503.1142.v1

is approximately the same, but the differences in intensities and peak widths are different. The main peak at around 3000 nm (hydrogen bonds) is present in all three cases which means that these structures are composed from water. A maximum wavelength shift between these structures is 66 nm. The intensities are different by three times in favor of the third derivative compared to the second derivative. The second peak at around 4700 nm is present in all three cases with a very small wavelength shift of 20 nm, with the intensity of the peak in the third derivative being more than 10 times higher than in the second derivative. The third peak at around 6100 nm is present in all three cases with a wavelength shift of about 160 nm, with the intensity of the peak in the third derivative being more than three times higher than in the second derivative.

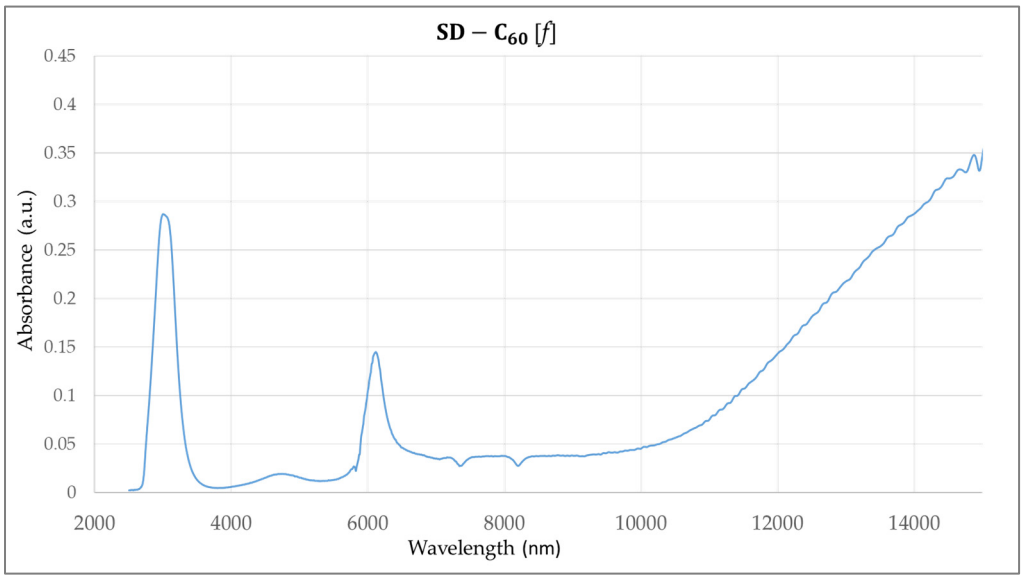

Figure 7. FTIR Spectra of SD-C_{60}-(f) with four peaks with given wavelengths and intensities: [3044 nm, 0.2852], [4740 nm,0.0192]. [6132 nm, 0.1431], [16000 nm,0.3500]. The peaks are not narrow, indicating that the structure's oscillatory processes are not of a high degree of coherence.

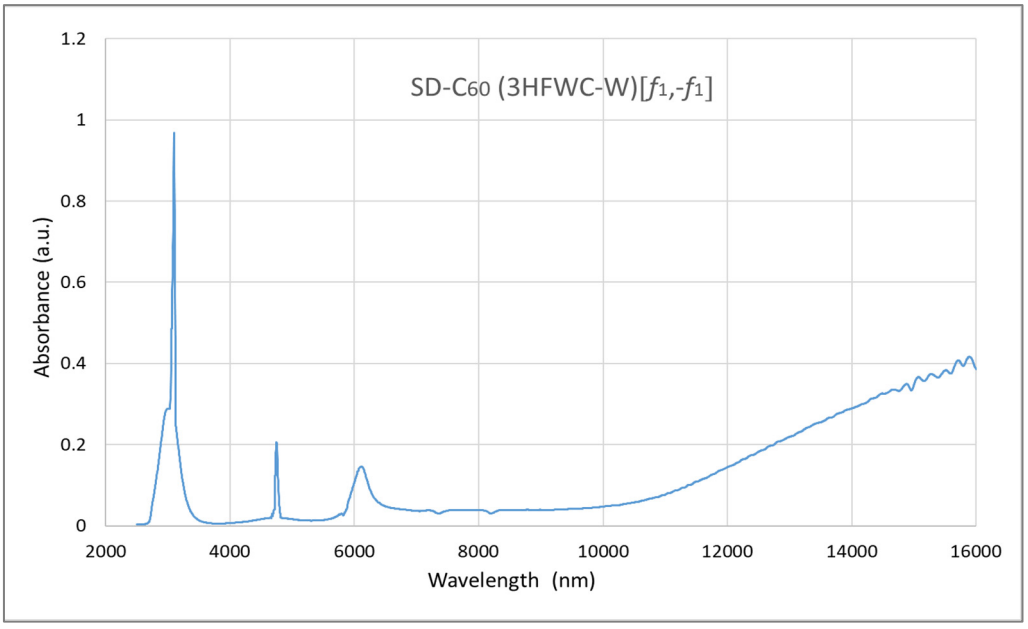

Figure 8. FTIR spectra of SD-C_{60}-(f_1,-f_1) with four peaks with given wavelengths and intensities: [3100 nm, 0.96325], [4748 nm, 0.2048], [6084 nm,0.1433], [16000 nm, 0.4000]. The first two peaks are narrow, which indicates a high degree of coherence.

 doi:10.20944/preprints202503.1142.v1

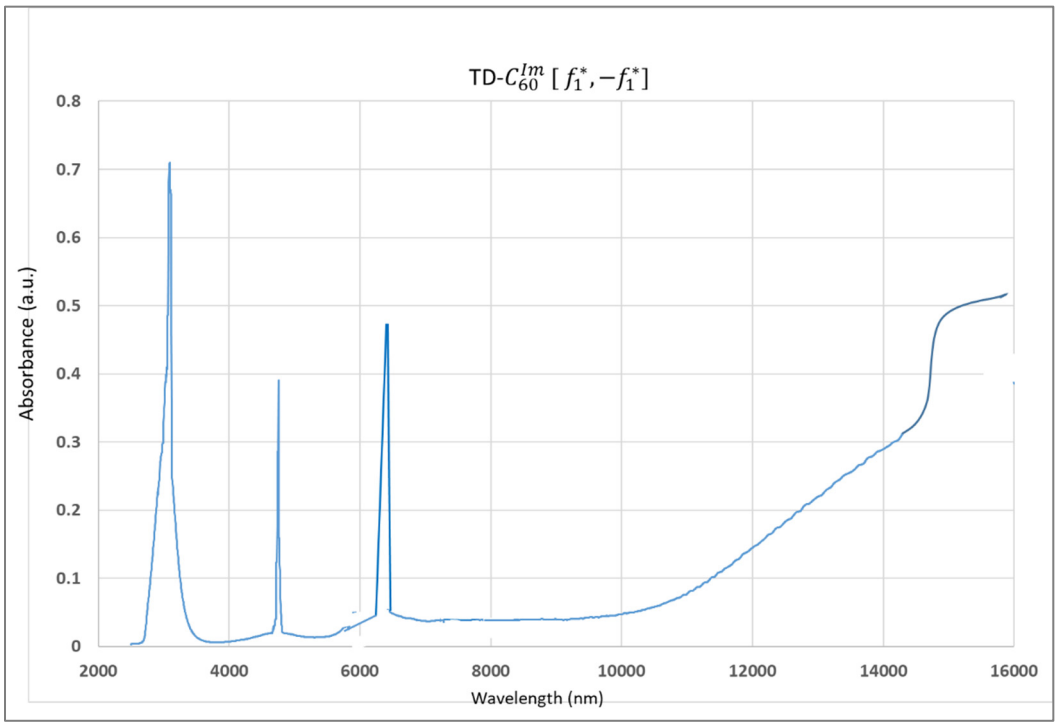

Figure 9. FTIR spectra of TD-C60-(f_1^x,- f_1^x) with four peaks with given wavelengths and intensities: [3088 nm, 0.7086], [4760 nm, 0.3884], [6244 nm,0.4813], [16000 nm, 0.5162]. The first three peaks are very narrow, which indicates a high degree of coherence.

3.4. MFM Spectra of SD-C60 and TD-C60 Derivative of C60

MFM spectra show hydrogen bonds in all five structures of C60 derivatives are present (Figure 10). MFM precisely determines the intensity of hydrogen bond dynamics. The intensity of paramagnetic spectra is very high, meaning that C60 derivatives are very rich in water molecules because they interact with the MFM tip (dipole-dipole interaction). The results prove the water molecules' presence and the intensity of water dynamics in all five structures of C60 derivatives. Blue lines (Figure 10) show moisture presence in the precursor. The intensity of hydrogen bond dynamics in the C60 derivatives is many times greater than in the case when it is only present moisture in FD-C60.

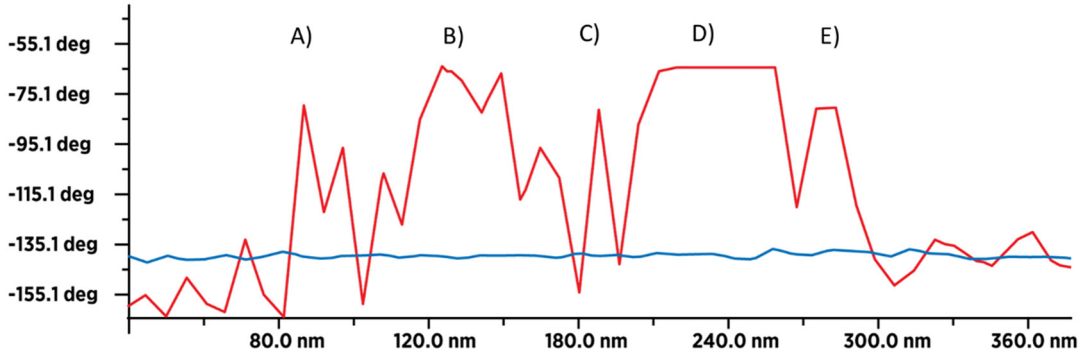

Figure 10. Magnetic Force Microscopy (MFM) diagram (scan size 360 nm) of the presence of hydrogen bonds in C60 derivatives (red line), while the blue line is the presence of moisture of the first derivative FD-C60 (fullerenol). As can be seen from the diagram, there are five basic structures of C60 derivatives: **A)** SD-C60 (3HFWC-[*f*]), **B**) SD-C60 (3HFWC-W[-f_1]), **C**) SD-C60 (3HFWC-W[f_1] (similar structure as *f*), **D)**TD-C60 ([f_1^*]), and **E)** TD-C60([-f_1^*] (structure notation of f_1,-f_1, f_1^*,-f_1^* is given on images, Figure 11).

 doi:10.20944/preprints202503.1142.v1

3.5. Yin-Yang Phenomenon of C_{60} Molecule Derivatives: Quantum-Classical Harmonic (QCH)Substance

The C_{60} molecule is both a classical and a quantum entity because it behaves as a particle and a wave [20]. It transfers its harmonized physical properties to the water layers around it, consisting of water molecules whose hydrogen bonds are also classical-quantum [12]. Through vibrational modes Φ,-ϕ,-Φ,ϕ its harmonized vibrational states are transferred to water, and it further transfers vibrations to biomolecules that have hydrogen bonds (DNA and proteins, such as collagen, microtubules, clathrin, actin, etc.).

The oscillatory magnetic field equation H (ωt) = A *cos* (ωt) + B *isin*(ωt) gives the possibility to make three types of derivatives of C_{60} molecules: 1, 2, and 3 (Figure 11). The first form of the second derivative of the C_{60} molecule (SD-C_{60}) is created under the influence of the magnetic oscillatory field of the reactor H(ωt)= $A_0 e^{i\pi\omega}$ (3HFWC or *f*) and the vibration of the C_{60} molecule. The second form of the second derivative of the C_{60} molecule (SD-C_{60} (3HFWC-W) or f_1,-f_1), which has two structures (f_1 and -f_1), is formed under the effect of the *Re* magnetic oscillatory field of the reactor H(ωt)=*Acos*(ωt), and the vibration of C_{60} molecules. The third derivative of C_{60} molecules (TD-C_{60} or f_1^*,-f_1^*) which also has two structures (f_1^* and -f_1^*), is created under the effect of the *Im* magnetic oscillatory field of the reactor H(ωt)= *B isin*, and the vibration of the C_{60} molecules.

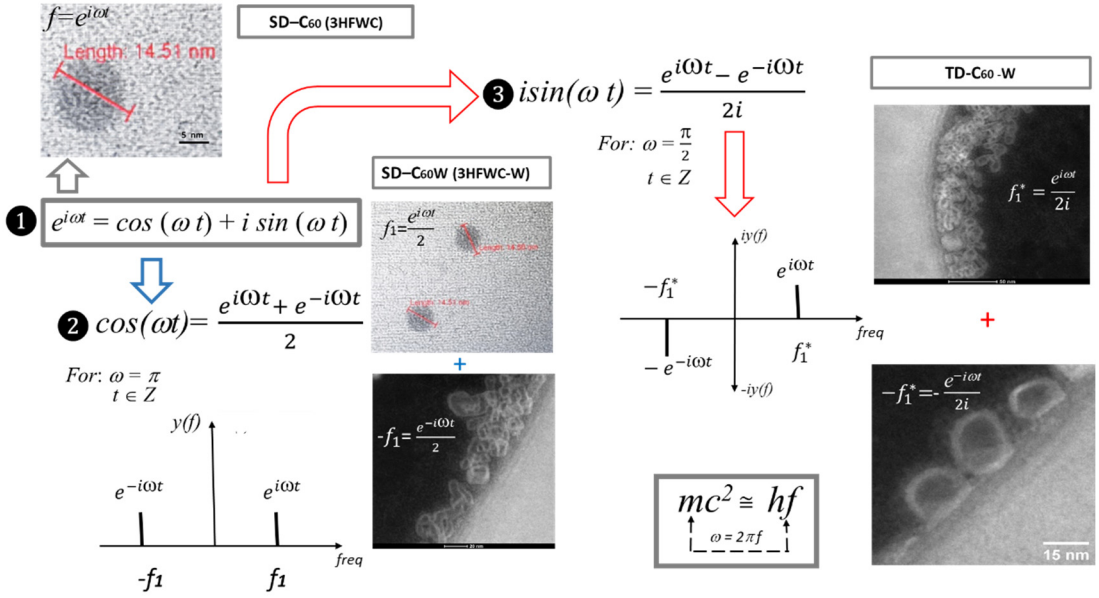

Figure 11. Summary schematic representation of SD-C_{60} and TD-C_{60} derivatives of C_{60} molecules. The second derivative SD-C_{60} has two forms SD-C_{60}-(*f*) or 3HFWC and SD-C_{60}-(f_1,-f_1) or 3HFWC-W. The first form is formed as an interaction of Φ vibration molecule C_{60} and the frequency (*f*) of the oscillatory magnetic field of the reactor. The second form of the derivative has two structures which are the result of the effect of the vibrational modes Φ and -ϕ of the C_{60} molecules on the water molecules in the reactor and the frequency of the *Re* oscillating magnetic field of the reactor f_1 and -f_1. The third derivative also has two harmonized structures that arise as a result of the effect of the vibrations of C_{60} molecules (-Φ, ϕ) and the frequencies of the *Im* oscillatory magnetic field of reactors f_1^* and -f_1^*.

In the system of icosahedral symmetry, to which C_{60} belongs, not only two paired eigenvalues Φ,-ϕ are harmonic, but also the system of two paired values (square:Φ,-ϕ,-Φ,ϕ) is harmonic. Because of such relationships, the system can be represented as the ancient Chinese *Yin-Yang* system: big *Yin*, small *yin*, big *Yang*, small *yang* (Figure 12 left).

The vibrational modes of the oscillatory magnetic field of the reactor are also matched according to the laws of harmony. The elements of Euler's formula $e^{i\omega\pi}$ (*cos*(ωt) and *isin*(ωt)) also form a harmonic logical square ($1/2e^{i\omega t}$, $1/2e^{-i\omega t}$, $e^{-i\omega t}/2i$, $-e^{-i\omega t}/2i$) as is the case with Yin-Yang (Figure 12, right).

Preprints.org (www.preprints.org) | NOT PEER-REVIEWED | Posted: 17 March 2025 doi:10.20944/preprints202503.1142.v1

These two *Yin-Yang* systems are the "heads or tails" of a coin based on the symmetry-harmony of the C_{60} molecule and the oscillatory magnetic field of the reactor that creates derivatives.

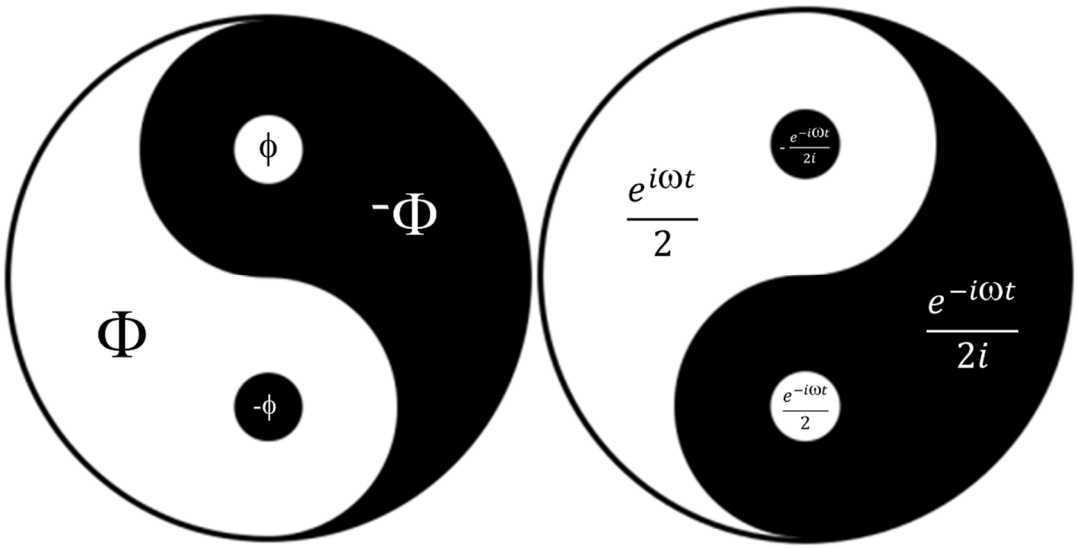

Figure 12. "Heads or tails" of symmetry-harmony of C_{60} molecule derivatives. The icosahedral symmetry of C_{60} contains four symmetry elements Φ,-ϕ,-Φ,ϕ which ensure the harmony of structural-energetic stability. Its harmony transfers to the surrounding water molecules via hydrogen bonds. Simultaneously, the process (reactor) generates four frequency modes f_1, $-f_1$, f_1^*, $-f_1^*$ (which generate water structures according to the same law as C_{60}). This is the Euler-Fibonacci-Kostić (EFK) principle because f_1, $-f_1$, f_1^*, $-f_1^*$ are elements of Euler's formula $e^{i\omega t} = cos(\omega t) + i\ sin\ (\omega t)$ and elements Φ,-ϕ,-Φ,ϕ are Fibonacci's pairs. At the same time, their unity ("heads or tails") is Kostić's coin solution, who said, "Harmony is the synthesis of symmetry, symmetry is the analysis of harmony" [21]. This is exactly what happens to the structure and energy of the hydrogen bonds according to the Penrose process of 3D tiling formation [16].

The presented Yin-Yang systems in the picture Figure 12 are not given symbolically but are real entities of C_{60} molecules and their derivatives. In the case of Figure 13 *right*, there is an interference of two electromagnetic waves (C_{60} and reactor) that interact and maintain a harmonized relationship (Yin-Yang) of their amplitudes in that interaction. There is a similar case in the biphoton experiment when the amplitude and phase structure make the image that can be detected as Yin-Yang order [22] (Supplement S4, Figure S3).

 doi:10.20944/preprints202503.1142.v1

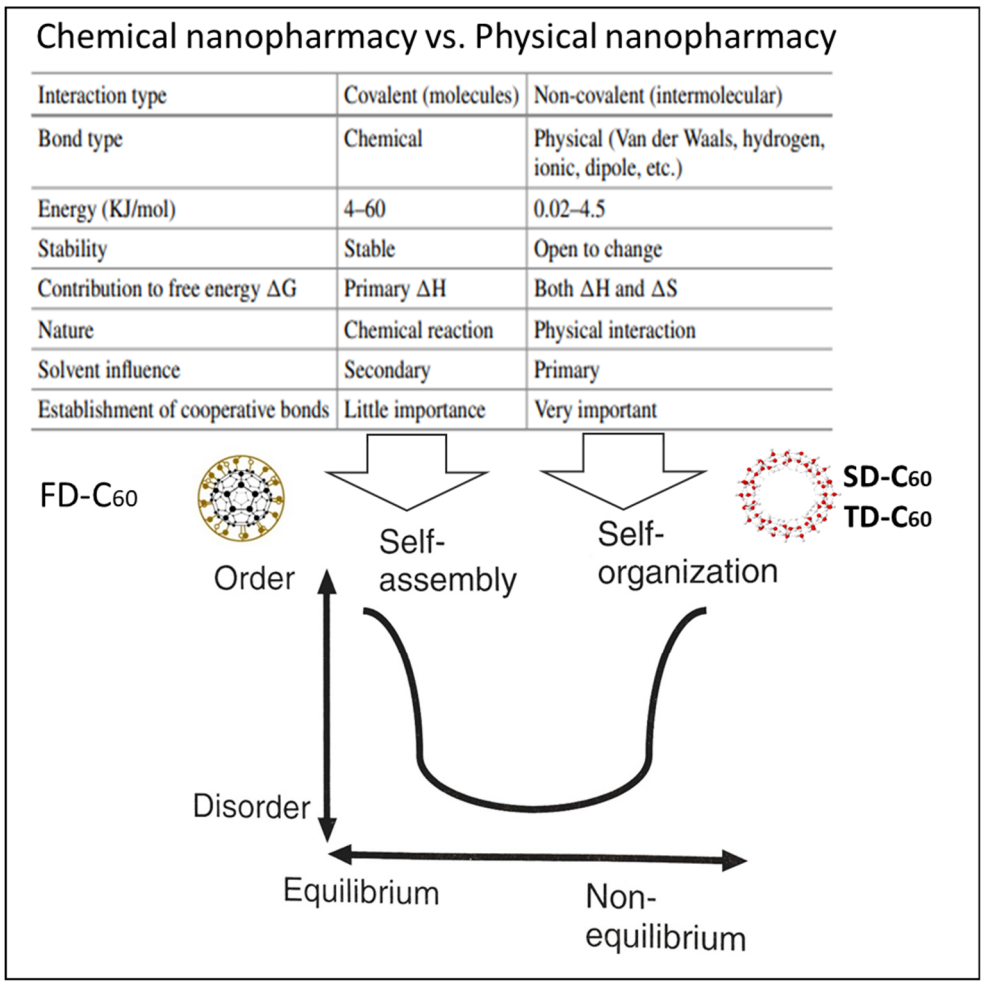

Figure 13. Presentation of similarities and differences of chemical and physical phenomena at the nano level (Chemical nanopharmacy vs. physical nanopharmacy). Solvent influence is very important, secondary means is not an active entity in process, and primary means it is an active entity **(**Adapted from [23,24]). A similar situation exists in biology: protein synthesis, for example, tubulin, is a self-assembly process (biochemical), while the polymerization of tubulin into microtubules and microtubules into centrioles is a self-organization process (biophysical).

4. Discussion

The three most important things are discussed in this section. First, what are the similarities and differences between chemical nanopharmacy and physical nanopharmacy, secondly, what effects of C_{60} derivatives have been achieved in biomedical research, and thirdly, what would be the further direction of research.

4.1. Physical Nanopharmacy vs. Chemical Nanopharmacy

Similarities and differences between chemical and physical nano pharmaceutics are given in Figure 13. Chemical approaches are based on covalent bonds and physical ones on non-covalent bonds. Chemical is a self-assembly process, while physical is a self-organizing process. In chemistry, enthalpy (ΔH) is important, while in physics, next to enthalpy, entropy (ΔS) is also important. While chemical entities (molecules, like C_{60} and $C_{60}(OH)_x$) are stable with small variations in conformational changes, layers of water molecules based on intermolecular interactions are prone to change, with the fact that in a given environment they return to a stable state because water, as the solvent, is an active factor in the process (primary solvent influence).

 doi:10.20944/preprints202503.1142.v1

4.2. Effects of C_{60} Molecule Derivatives in Biomedical Application

Polyhydroxylated fullerenes (fullerenols) or FD-C_{60} have attracted great interest in recent years as promising candidates for cancer therapy due to their exceptional properties, such as high water solubility, biocompatibility, biodegradability, and rapid elimination from the body. These nanomaterials are particularly valuable for cancer treatment because they can inhibit tumor growth and enhance the immune response against cancer cells [25]. Fullerenols (FD-C_{60}) are also known for their ability to act as photosensitizers (PS), i.e., molecules that can be activated by specific wavelengths of light, providing an additional option for cancer treatment through phototherapy [26,27]. Although fullerenols are generally known for their antioxidant properties [28,29], they can act as prooxidants upon photoexcitation due to the generation of ROS [30,31], which makes them potential candidates for cancer phototherapy.

Our recent studies have demonstrated the potential of the second fullerene derivative, 3HFWC or SD-C_{60} as an antitumor agent in melanoma in vitro and in vivo models [32,33] in combination with light treatment. Specifically, cells exposed to 3HFWC (SD-C_{60}) were irradiated with incoherent, phase-shifted, unsynchronized, polychromatic, hyperpolarized light (HPL) (Bioptron-2 device, Bioptron AG, Wollerau, Switzerland) [34]. The nanophotonic fullerene-filtering light of this device allowed the emission of a broad spectrum of wavelengths (light from 400 to 1100 nm, and infrared (IR) irradiation from 5000-15000 nm, with characteristic peaks at 5811 nm, 8732 nm, and 13300 nm). In vitro experiments performed with both primary cells and melanoma cell lines of different grades and invasiveness (low-grade B16 and high-grade B16-F10 mouse cells and human A375 cells), demonstrated the selective anticancer effect of 3HFWC. This effect was attributed to the induction of senescence and/or differentiation towards the melanocytic phenotype. Electron microscopy analyses also showed that 3HFWC was efficiently internalized by the cells, indicating this process is an important step in the reprogramming of cancer cells [32]. Subsequently, the anticancer effect of 3HFWC (SD-C_{60}) was confirmed in vivo using a syngeneic mouse melanoma model. Mice were treated with 3HFWC via drinking water (0.145 mg/mL, *ad libitum*) after tumor induction alone or in combination with HPL irradiation of animals (2 x 20 min daily). Again, 3HFWC-induced senescence and differentiation of melanoma cells were observed. Senescent cells were larger with enlarged nuclei, more lipid droplets, increased lysosomal activity, and altered mitochondrial morphology. On the other hand, cells that had undergone melanocytic differentiation had smaller, heterochromatic nuclei, increased melanin production, and well-developed dendrites with mature melanosomes [32,33]. Cell senescence is a stable state characterized by cell cycle arrest, and is considered as a response to cell damage caused by various stressors [35,36]. This process is considered beneficial in cancer therapy as it reduces the malignant potential of neoplastic cells in contrast to traditional cytotoxic approaches such as chemotherapy and radiotherapy, [37–39]. Inducing senescence in cancer cells may be beneficial as it reduces their aggressiveness and regulates the tumor microenvironment (TME). Senescent cells are known to secrete proinflammatory cytokines and matrix metalloproteinases [40,41], which affect the cancer cells and other cells and extracellular matrix components within the TME [42,43]. Senescent cancer cells can recruit immune cells to the site, and thus promote antitumor immune surveillance [44–48]. In melanoma models, treatment with 3HFWC (SD-C_{60}), especially in combination with HPL irradiation, stimulated the infiltration of tumor-suppressive immune cells such as CD8+ cytotoxic T lymphocytes. In contrast, the presence of tumor-promoting immune cells such as T regulatory cells, myeloid-derived suppressor cells, and M2 macrophages was reduced in TME [33]. These results suggest that 3HFWC also has immunomodulatory effects and thus converts “cold” (non-inflamed) tumors into “warm” (inflamed) tumors that might respond better to immunotherapy [49–52].

In summary, the combination of 3HFWC treatment and HPL irradiation could represent a novel approach to cancer therapy, not only by directly reprogramming and destroying tumor cells but also by activating an immune response that attacks and eliminates the remaining neoplastic cells. This dual mechanism of action-cellular reprogramming and activation of the immune response distinguishes it from conventional cytotoxic treatments. Although HPL irradiation enhanced the

 doi:10.20944/preprints202503.1142.v1

effect of 3HFWC, it did not induce the same strong oxidative stress typically associated with PDT. This suggests that the combined treatment works via a different mechanism, possibly through the organization of water dipoles around the 3HFWC molecules, which enhances their anti-cancer effect without causing significant cytotoxicity [32].

Further studies on the prophylactic use of 3HFWC (SD-C_{60}) as well as its combination with other treatment modalities are needed to fully understand its potential as a cancer therapy. Initial results suggest that administration of 3HFWC (SD-C_{60}) after tumor induction is more effective than preventive treatment, which could impair the early antitumor immune response [53,54]. Toxicity studies in normal cells did not show severe systemic toxicity, although mild liver and kidney damage was observed in some cases, which warrants further investigation to determine the optimal dosage and treatment duration before potential use in humans [33].

Compared to the previously described 3HFWC (SD-C_{60}-f, Figure 4) compound, the improved formulation labeled 3HFWC-W (SD-C_{60}-f_1,-f_1), (Figure 5) showed a significantly amplified potential to limit melanoma cell growth in vitro. Despite this enhanced activity, the mechanism of action remained unchanged as it primarily induced cellular senescence and did not lead to cell death [33].

The synthesis of SD-C_{60}-f (3HFWC-W) with a magnetic field of the type H(ωt) = Acos(ωt) is similar to stepwise oscillatory circuits of DNA molecules with current law $I = 5.2e^{-0.005t}cos(0.068t)$, where A= $5.2e^{-0.005t}$ and the angular velocity of the oscillation ω = 0.068 [55]. The under-damped oscillation with parameters C= 0.02pF, L= 0.01H, and R=100 a frequency value, according to equation $\omega=\sqrt{\frac{1}{LC}-\frac{R^2}{4L^2}}$, is about 2×10^{10} s^{-1} (Supplement S5 (S5F4). It is a similar value to the ^{13}C-NMR experimental result of C_{60} a rotational diffusion constant D=1.8×10^{10} s^{-1} [56] (Supplement S6 (S6F5)).

4.3. The Further Direction of Research

Bearing in mind what was said in Sections 3.4 and 4.2, it is necessary: (1) to continue with the chemical-physical characterization of the second (SD-C_{60}-f_1,-f_1)[3HFWC-W] and third derivative (TD-C_{60}) of the C_{60} molecule, (2) to examine the biomedical effects of the second derivative C_{60}/(f_1,-f_1) and the third derivative C_{60}/(f_1*,-f_1*), individually, and (3) promising biomedical research of *Quantum-classical medical substance (QCMS)* which is a harmonized unity (synergy) of the second derivative SD-C_{60}/(f_1,-f_1) and the third C_{60}(f_1*,- f_1*) derivatives (QCH =(f_1,-f_1)/(f_1*,- f_1*), Yin-Yang substance, Figure 12, right).

5. Conclusions

The task of science in general, and pharmacy in particular, is to review existing knowledge and technological solutions and to propose, based on theoretical and experimental knowledge, new methods, techniques, and products that contribute to the improvement of human health. The results presented in this paper support the fact that in the field of pharmacy, especially nanopharmacy, there is a possibility of improving human health by using not only chemical (FD-C_{60}) but also physical methods (SD-C_{60} and TD-C_{60}). A particularly important area is hydrogen bonds, which are the most widespread interactions in biological systems because they are an integral part of the intermolecular interactions of water, which is 60-70% of the organism, DNA (A=T, C=G), proteins (O...H and N.. .H) which make up about 16% of the structure of the human organism.

The paper presents the method of obtaining derivatives of C_{60} molecules and their characterization using FTIR, TEM, and AFM/MFM. It was shown that the size of the derivatives is about 15 nm and that they are rich in water molecules arranged in water layers with a high degree of vibrational coherence.

A brief overview of the initial biomedical research on the application of derivatives of C_{60} molecules indicates that these nano physical pharmacological substances have good effects in the treatment of cancer, Alzheimer's, and other diseases. To further test the existing derivatives of the C_{60} molecule, it is necessary to conduct a biomedical study to determine the effects of the newly obtained

 doi:10.20944/preprints202503.1142.v1

integral substance of C_{60} derivatives *Quantum-classical harmonic (QCH)* substance which is a Yin-Yang harmonized unity of the second $C_{60}/(f_1,-f_1)$ and the third $C_{60}(f_1^*,-f_1^*)$ derivatives.

6. Patents

1. Koruga, D. Composition of Matter Containing Harmonized Hydroxyl Modified Fullerene Substance. U.S. Patent 8,058,483 B2, 15 November 2011.
2. Koruga, D. Compositions Comprising Hyper Harmonised Hydroxyl Modified Fullerene Substances. International Patent WO 2021/110234 A1, 10 June 2021.

Supplementary Materials: The following supporting information can be downloaded at the website of this paper posted on Preprints.org, Supplement S1, Figure S1: Order of water hydrogen bonds, Supplement S2, Table S1: Icosahedral symmetry group, Supplement S3, Figure S2: Real *Re* and imaginary *Im* frequency range of C_{60}, Supplement S4, Figure S3: Yin-Yang in biphoton experiments. Supplement S5, Figure S4, The hydrogen bonds oscillatory circuit of a DNA. Supplement S6, Figure S5 (S6F5): C_{60} rotation (^{13}C-NMR)

Author Contributions: For research articles with several authors, a short paragraph specifying their individual contributions must be provided. The following statements should be used: "Conceptualization, Djuro Koruga and Lidija Matija.; methodology, Djuro Koruga, validation, Aleksandra Dinić; investigation, Djuro Koruga, Dietmar Kuhn, Lidija Matija, Ivana Stanković. resources Lidija Matija; data curation, Aleksandra Dinić; writing—original draft preparation, Djuro Koruga; writing—review and editing, Lidija Matija, Ivana Stanković; visualization, Djuro Koruga; supervision, Lidija Matija.; project administration, Aleksandra Dinić.; funding acquisition, Djuro Koruga. All authors have read and agreed to the published version of the manuscript.

Funding: This research received no external funding.

Institutional Review Board Statement: Not applicable

Informed Consent Statement: Not applicable. Pharmaceutics 2025, 17, 71 25 of 28

Data Availability Statement: The data presented in this study are available on request from the corresponding author.

Acknowledgments: The authors would like to thank Philipp Müller, Analytical and Material Science, the University in Heidelberg, Germany, for his collaboration in the characterization of C_{60} molecule derivatives using TEM.

Conflicts of Interest: The authors declare no conflicts of interest.

References

1. Keerti Jain, Neelesh Kumar Mehra, Narendra Kumar Jain, Potentials and emerging trends in nanopharmacology, Current Opinion in Pharmacology, Volume 15, April 2014, Pages 97-106, https://doi.org/10.1016/j. coph.2014. 01.006
2. Diaz,J.E.M., Nanotechnology in pharmacology: Advances and Applications in Drag Delivery, Joural of Pharmacology and Clinical Research, Mini Reviw, 9(5) JPCR.MS.ID.555773 (2023), DOI: 10.19080/JPCR.2023.09.555773
3. Gaurav Tiwari, Ruchi Tiwari, Birendra Sriwastawa, L Bhati, S Pandey, P Pandey, Saurabh K Bannerjee, Drug delivery systems: An updated review, International Journal of Pharmaceutical Investigation | January 2012 | Vol 2 | Issue 1, DOI: 10.4103/2230-973X.96920.
4. Chiang, L.Y.; Upasani, R.B.; Swirczewski, J.W. Process of Forming Polysubstituted Fullerenes .U.S. Patent 5,177,248, 5 January 1993.
5. Sayes, C.M.; Fortner, J.D.; Guo, W.; Lyon, D.; Boyd, A.M.; Ausman, K.D.; Tao, Y.J.; Sitharaman, B.; Wilson, L.J.; Hughes, J.B.; et al. The differential cytotoxicity of water-soluble fullerenes. *Nano Lett.* **2004**, *4*, 1881–1887. https://doi.org/10.1021/nl0489586.

 doi:10.20944/preprints202503.1142.v1

6. Isakovic, A.; Markovic, Z.; Todorovic-Markovic, B.; Nikolic, N.; Vranjes-Djuric, S.; Mirkovic, M.; Dramicanin, M.; Harhaji, L.; Raicevic, N.; Nikolic, Z.; et al. Distinct cytotoxic mechanisms of pristine versus hydroxylated fullerene. *Toxicol. Sci.* **2006**, *91*,173–183. https://doi.org/10.1093/toxsci/kfj127.
7. Bogdanović, G.; Kojić, V.; Đorđević, A.; Čanadanović-Brunet, J.; Vojinović-Miloradov, M.; Baltić, V.V. Modulating activity of fullerol C60(OH)22 on doxorubicin-induced cytotoxicity. *Toxicol. Vitr.* **2004**, *18*, 629–637. https://doi.org/10.1016/j.tiv.2004.02.010.
8. Jiao, F.; Liu, Y.; Qu, Y.; Li, W.; Zhou, G.; Ge, C.; Li, Y.; Sun, B.; Chen, C. Studies on anti-tumor and antimetastatic activities of fullerenol in a mouse breast cancer model. *Carbon* **2010**, *48*, 2231–2243. https://doi.org/10.1016/j.carbon.2010.02.032.
9. Liu, Y.; Jiao, F.; Qiu, Y.; Li, W.; Qu, Y.; Tian, C.; Li, Y.; Bai, R.; Lao, F.; Zhao, Y.; et al. Immunostimulatory properties and enhanced TNF- α mediated cellular immunity for tumor therapy by C60(OH) 20 nanoparticles. *Nanotechnology* **2009**, *20*, 415102. https://doi.org/10.1088/0957-4484/20/41/415102.
10. Yamawaki, H.; Iwai, N.; Saito, K.; Okada, M.; Hara, Y. Cytotoxicity of water-soluble fullerene in vascular endothelial cells. *Am.J. Physiol. Cell Physiol.* **2006**, *290*, C1495–C1502. https://doi.org/10.1152/ajpcell.00481.2005.
11. Johnson-Lyles, D.N.; Peifley, K.; Lockett, S.; Neun, B.W.; Hansen, M.; Clogston, J.; Stern, S.T.; McNeil, S.E. Fullerenol cytotoxicity in kidney cells is associated with cytoskeleton disruption, autophagic vacuole accumulation, and mitochondrial dysfunction. *Toxicol. Appl. Pharmacol.* **2010**, *248*, 249–258. https://doi.org/10.1016/j.taap.2010.08.008.
12. Isaacs, E.D., Covalence of the hydrogen bond in ice: A direct X-ray measurement, *Physical Review Letters*, 82, pp. 600-603, 1999.
13. Dresselhous, M.S.; Dresselhous, G.; Eklund, P.C. *Science of Fullerenes and Carbon Nanotubes*; Elsevier BV: Amsterdam, The Netherlands,1996
14. Koruga, D. Composition of Matter Containing Harmonized Hydroxyl Modified Fullerene Substance. U.S. Patent 8,058,483 B2, 15 November 2011.
15. Koruga, D. Compositions Comprising Hyper Harmonised Hydroxyl Modified Fullerene Substances. International Patent WO 2021/110234 A1, 10 June 2021.
16. Matija, L.; Stanković, I.; Purić, M.; Miličić, M.; Maksimović-Ivanić, D.; Mijatovic, S.; Krajnović, T.; Koruga, D. The Second Derivative of Fullerene C_{60} (SD-C_{60}) and Biomolecular Machinery of Hydrogen Bonds: Water-Based Nanomedicine. *Micromachines* **2023**, *14*, 2152. https://doi.org/10.3390/ mi14122152.
17. Djuro Koruga, Ivana Stanković, Lidija Matija, Dietmar Kuhn, Bastian Christ, Sofia Dembski, Nenad Jevtić, Jelena Janać, Vladimir Pavlović and Bart De Wever, Comparative Studies of the Structural and Physicochemical Properties of the First Fullerene Derivative FD-C_{60} (Fullerenol) and Second Fullerene Derivate SD-C_{60} (3HFWC), *Nanomaterials* **2024**, *14*(5), 480; https://doi.org/10.3390/nano14050480
18. Jeffrey. A. George, An Introduction to hydrogen bonding, Oxford University Press, New York, 1997.
19. Koruga, Dj., Qi Engineering: Classical-Quantum Biophysics, Acupuncture and Chaakras, Grafopen, Belgrade, 2024, ISBN 978-86-83615-44-5.
20. Markus Arndt, Olaf Nairz, Julian Vos-Andreae, Claudia Keller, Gerbrand van der Zouw & Anton Zeilinger, Wave-particle duality of C_{60} molecules, *Nature*, VOL 401, 680-681,1999.
21. Laza Kostić, *The Basic Principle,* The City Library "Karlo Bjelicki", Sombor, 2015
22. Zia, D., Dhegihan, N., D'Errico, A., Sciarrino, F., Karimi, E., (2023). Interferometric imaging of amplitude and phase of spatial biphoton states, *Nature Photonics,* 1009–1016, DOI:10.1038/s41566-023-01272-3.
23. Mannsoori G.A, Principles of Nanotechnology: Molecular Based Study of Condensed Matter in Small Systems, World Scientific, New Jersey, 2005.
24. 24 Malsch, N.H., Biomedical Nanotechnology, CRC Press-Taylor and Francis, Boca Raton, 2005.
25. Krishna, V., A. Singh, P. Sharma, N. Iwakuma, Q. Wang, Q. Zhang, J. Knapik, H. Jiang, S. R. Grobmyer, B. Koopman, and B. Moudgil. 'Polyhydroxy fullerenes for non-invasive cancer imaging and therapy', Small, 6: 2236-41. 2010
26. Chen, A., S. R. Grobmyer, and V. B. Krishna. 'Photothermal Response of Polyhydroxy Fullerenes', ACS Omega, 5: 14444-50, 2020.

 doi:10.20944/preprints202503.1142.v1

27. Pickering, K. D., and M. R. Wiesner. 2005. 'Fullerol-sensitized production of reactive oxygen species in aqueous solution', Environ Sci Technol, 39: 1359-65.
28. Castro, E., A. Hernandez Garcia, G. Zavala, and L. Echegoyen. 2017. 'Fullerenes in Biology and Medicine', J Mater Chem B, 5: 6523-35.
29. Grebowski, Jacek, Adrian Konopko, Anita Krokosz, Gino A. DiLabio, and Grzegorz Litwinienko. 2020. 'Antioxidant activity of highly hydroxylated fullerene C60 and its interactions with the analogue of α-tocopherol', Free Radical Biology and Medicine, 160: 734-44.
30. Mroz, P., A. Yaroslavsky, G. B. Kharkwal, and M. R. Hamblin. 2011. 'Cell death pathways in photodynamic therapy of cancer', Cancers (Basel), 3: 2516-39.
31. Fernandes, Neha Benedicta, Raghavendra Udaya Kumar Shenoy, Mandira Kashi Kajampady, Cleona E. M. Dcruz, Rupesh K. Shirodkar, Lalit Kumar, and Ruchi Verma. 2022. 'Fullerenes for the treatment of cancer: an emerging tool', Environmental Science and Pollution Research, 29: 58607-27.
32. Markelic, M., D. Draca, T. Krajnovic, Z. Jovic, M. Vuksanovic, D. Koruga, S. Mijatovic, and D. Maksimovic-Ivanic.' Combined Action of Hyper-Harmonized Hydroxylated Fullerene Water Complex and Hyperpolarized Light Leads to Melanoma Cell Reprogramming In Vitro', Nanomaterials (Basel), 2022;12(8):1331. doi:10.3390/nano12081331
33. Markelic, M., M. Mojic, D. Bovan, S. Jelaca, Z. Jovic, M. Puric, D. Koruga, S. Mijatovic, and D. Maksimovic-Ivanic. 2023. 'Melanoma Cell Reprogramming and Awakening of Antitumor Immunity as a Fingerprint of Hyper-Harmonized Hydroxylated Fullerene Water Complex (3HFWC) and Hyperpolarized Light Application In Vivo', Nanomaterials (Basel), . 2023;13(3):372. doi:10.3390/nano13030372
34. Koruga,D., Hyperpolarized Light: Fundamentals of Nanobiomedical Phptonics, Zepter Book World, Belgrade 2018, ISBN:78-86-7494-136-2.
35. Hernandez-Segura, A., J. Nehme, and M. Demaria. 2018. 'Hallmarks of Cellular Senescence', Trends Cell Biol, 28: 436-53.
36. Gorgoulis, V., P. D. Adams, A. Alimonti, D. C. Bennett, O. Bischof, C. Bishop, J. Campisi, M. Collado, K. Evangelou, G. Ferbeyre, J. Gil, E. Hara, V. Krizhanovsky, D. Jurk, A. B. Maier, M. Narita, L. Niedernhofer, J. F. Passos, P. D. Robbins, C. A. Schmitt, J. Sedivy, K. Vougas, T. von Zglinicki, D. Zhou, M. Serrano, and M. Demaria. 2019. 'Cellular Senescence: Defining a Path Forward', Cell, 179: 813-27.
37. Campisi, J. 2013. 'Aging, cellular senescence, and cancer', Annu Rev Physiol, 75: 685-705.
38. Collado, M., and M. Serrano. 2010. 'Senescence in tumours: evidence from mice and humans', Nat Rev Cancer, 10: 51-7.
39. Collado, M., and M. Serrano. 2010. 'Senescence in tumours: evidence from mice and humans', Nat Rev Cancer, 10: 51-7
40. Arima, Y., H. Nobusue, and H. Saya. 2020. 'Targeting of cancer stem cells by differentiation therapy', Cancer Sci, 111: 2689-95.
41. Coppé, Jean-Philippe, Pierre-Yves Desprez, Ana Krtolica, and Judith Campisi. 2010. 'The Senescence-Associated Secretory Phenotype: The Dark Side of Tumor Suppression', Annual Review of Pathology: Mechanisms of Disease, 5: 99-118.
42. Birch, J., and J. Gil. 2020. 'Senescence and the SASP: many therapeutic avenues', Genes Dev, 34: 1565-76.
43. El-Deiry, W. S., B. Taylor, and J. W. Neal. 2017. 'Tumor Evolution, Heterogeneity, and Therapy for Our Patients With Advanced Cancer: How Far Have We Come?', Am Soc Clin Oncol Educ Book, 37: e8-e15.
44. Baghban, R., L. Roshangar, R. Jahanban-Esfahlan, K. Seidi, A. Ebrahimi-Kalan, M. Jaymand, S. Kolahian, T. Javaheri, and P. Zare. 2020. 'Tumor microenvironment complexity and therapeutic implications at a glance', Cell Commun Signal, 18: 59.
45. Wang, Liqin, Lina Lankhorst, and René Bernards. 2022. 'Exploiting senescence for the treatment of cancer', Nature Reviews Cancer, 22: 340-55.
46. Faget, D. V., Q. Ren, and S. A. Stewart. 2019. 'Unmasking senescence: context-dependent effects of SASP in cancer', Nat Rev Cancer, 19: 439-53.
47. Ruscetti, M., J. Leibold, M. J. Bott, M. Fennell, A. Kulick, N. R. Salgado, C. C. Chen, Y. J. Ho, F. J. Sanchez-Rivera, J. Feucht, T. Baslan, S. Tian, H. A. Chen, P. B. Romesser, J. T. Poirier, C. M. Rudin, E. de Stanchina,

 doi:10.20944/preprints202503.1142.v1

E. Manchado, C. J. Sherr, and S. W. Lowe. 2018. 'NK cell-mediated cytotoxicity contributes to tumor control by a cytostatic drug combination', Science, 362: 1416-22.

48. Kang, T. W., T. Yevsa, N. Woller, L. Hoenicke, T. Wuestefeld, D. Dauch, A. Hohmeyer, M. Gereke, R. Rudalska, A. Potapova, M. Iken, M. Vucur, S. Weiss, M. Heikenwalder, S. Khan, J. Gil, D. Bruder, M. Manns, P. Schirmacher, F. Tacke, M. Ott, T. Luedde, T. Longerich, S. Kubicka, and L. Zender. 2011. 'Senescence surveillance of pre-malignant hepatocytes limits liver cancer development', Nature, 479: 547-51.
49. Ruscetti, M., J. P. th Morris, R. Mezzadra, J. Russell, J. Leibold, P. B. Romesser, J. Simon, A. Kulick, Y. J. Ho, M. Fennell, J. Li, R. J. Norgard, J. E. Wilkinson, D. Alonso-Curbelo, R. Sridharan, D. A. Heller, E. de Stanchina, B. Z. Stanger, C. J. Sherr, and S. W. Lowe. 2020. 'Senescence-Induced Vascular Remodeling Creates Therapeutic Vulnerabilities in Pancreas Cancer', Cell, 181: 424-41.e21.
50. O'Donnell, Jake S., Michele W. L. Teng, and Mark J. Smyth. 2019. 'Cancer immunoediting and resistance to T cell-based immunotherapy', Nature Reviews Clinical Oncology, 16: 151-67.
51. Bonaventura, Paola, Tala Shekarian, Vincent Alcazer, Jenny Valladeau-Guilemond, Sandrine Valsesia-Wittmann, Sebastian Amigorena, Christophe Caux, and Stéphane Depil. 2019. 'Cold Tumors: A Therapeutic Challenge for Immunotherapy', Frontiers in Immunology,2019;10. doi:10.3389/fimmu.2019.00168
52. Duan, Q., H. Zhang, J. Zheng, and L. Zhang. 2020. 'Turning Cold into Hot: Firing up the Tumor Microenvironment', Trends Cancer, 6: 605-18.
53. Maleki Vareki, S. 2018. 'High and low mutational burden tumors versus immunologically hot and cold tumors and response to immune checkpoint inhibitors', J Immunother Cancer, 2018;6(1):157. doi:10.1186/s40425-018-0479-7
54. Mijatovic, S., A. Savic-Radojevic, M. Pljesa-Ercegovac, T. Simic, F. Nicoletti, and D. Maksimovic-Ivanic. 2020. 'The Double-Faced Role of Nitric Oxide and Reactive Oxygen Species in Solid Tumors', Antioxidants (Basel), 2020;9(5):374. doi:10.3390/antiox9050374
55. Kotsafti, A., M. Scarpa, I. Castagliuolo, and M. Scarpa. 2020. 'Reactive Oxygen Species and Antitumor Immunity-From Surveillance to Evasion', Cancers (Basel), 2020;12(7):1748. doi:10.3390/cancers12071748
56. Kunming, Xu, Stepwise oscillatory circuits of DNA molecules, J Biol Phys 35, 223-230, 2009, DOI:10.1007/s10867-009-9149-9
57. Johnson, R.D.; Yannoni, C.S.; Dorn, H.C.; Salem, J.R.; Bethune, D.S. C_{60} Rotation in the Solid State: Dynamics of a Faceted Spherical Top. Science 1992, 255, 1235–1238.
58. Matija LR, Stankovic IM, Puric M, Miličić M, Maksimović-Ivanić D, Mijatovic S, Krajnović T, Gordic V, Koruga DL. The Second Derivative of Fullerene C_{60} (SD-C60) and Biomolecular Machinery of Hydrogen Bonds: Water-Based Nanomedicine. Micromachines. 2023; 14(12):2152. https://doi.org/10.3390/mi14122152
59. Kettle, S.F.A., Symmetry and structure, John Willey and Sons, Chichester, 1995